

Cover Page



Universiteit Leiden



The handle <http://hdl.handle.net/1887/20840> holds various files of this Leiden University dissertation.

**Author:** Eldik, Willemijn van

**Title:** The role of CHAP in muscle development, heart disease and actin signaling

**Issue Date:** 2013-04-25



# Chapter 4

**Z-disc protein CHAPb induces cardiomyopathy and diastolic dysfunction**

Willemijn van Eldik, Abdelaziz Beqqali, Brigit den Adel, Jantine Monshouwer-Kloots, Daniela Salvatori, Saskia Maas, Nicky Boontje, Jolanda van der Velden, Paul Steendijk, Christine Mummery and Robert Passier



## Abstract

Cytoskeletal Heart-enriched Actin-associated Protein (CHAP) is a recently discovered Z-disc protein, which we found to be important for cardiac development. Here we studied the function of its two isoforms, resulting from alternative splicing of the *Chap* gene, in adult mouse hearts.

To determine the function of the “adult” CHAPa and “fetal” CHAPb isoforms through transgenic (Tg) overexpression specifically in mouse heart.

Two CHAPa and three CHAPb Tg founder lines were generated in which CHAP was driven by the myosin heavy chain (MHC) promoter. CHAPa Tg mice displayed normal cardiac function and phenotype, whereas CHAPb Tg mice showed mild cardiac hypertrophy, interstitial fibrosis and enlargement of the left atrium at 3 months of age, which was more pronounced by 6 months. Morphological cardiac hypertrophy and fibrosis were confirmed by evidence of activation of the hypertrophic gene program (*Nppa*, *Nppb*, *Myh7*) and increased expression of several collagens, respectively. Connexin40 and 43 were also downregulated in the left atrium, which was associated with delayed atrial conduction. CHAPb Tg hearts displayed both systolic and diastolic dysfunction partly caused by impaired sarcomere function evident from a reduced force generating capacity of single cardiomyocytes. Impaired cardiac function of CHAPb Tg mice coincided with activation of the actin-signaling pathway leading to the formation of stress fibers.

This study demonstrated that the fetal isoform CHAPb can initiate progression towards cardiac hypertrophy, which is accompanied by delayed atrial conduction and diastolic dysfunction. CHAP may thus be a novel candidate gene for familial cardiomyopathy.

## Introduction

Cardiac hypertrophy is an important determinant of cardiac disease. In pathological cardiac hypertrophy the increase in heart size is initially a compensatory mechanism, which eventually leads to impaired cardiac function and progression to heart failure<sup>1-3</sup>. Cardiac hypertrophy has various causes, which include responses to local environmental changes, such as myocardial infarction, pressure or volume overload and valvular defects, or by an intrinsic genetic defect that affects the cardiomyocyte directly and is referred to as familial hypertrophic and dilated cardiomyopathy (HCM and DCM, respectively). Besides cardiac hypertrophy, familial cardiomyopathy is also characterized by systolic and/or diastolic dysfunction, myofibrillar disarray and interstitial fibrosis. Several mutations in a relatively small group of genes have been associated with HCM and DCM. Whereas in HCM mutations predominantly interfere with proteins that are crucial for force generation, in DCM mutations affect proteins that play a role in force transmission from the sarcomere to the cytoskeleton<sup>4</sup>. Despite the increase in genetic associations with familial cardiomyopathies, our understanding of molecular regulation and signal pathways involved in familial cardiomyopathy (FCM) is still limited.

Recently, we discovered a novel protein that we called Cytoskeletal Heart-enriched Actin-associated Protein (CHAP)<sup>5,6</sup>, which is predominantly expressed in mouse striated muscle and localized at the Z-disc of sarcomeres. CHAP interacts with other Z-disc proteins, including  $\alpha$ -actinin-2, the major component of the Z-disc<sup>6</sup>. Two CHAP isoforms have been identified as a result of alternative splicing: CHAPa, expressed in adult mouse striated muscles, is the longer isoform, containing an N-terminal PDZ and a nuclear localization signal (NLS), whilst CHAPb is shorter and lacks the PDZ domain. CHAPb is predominantly expressed during early cardiac and skeletal muscle development and is downregulated in adult mouse tissues. Interestingly, we observed a perinatal switch in splice variant expression from the fetal CHAPb to the adult CHAPa isoform<sup>6</sup>. Zebrafish and chick orthologues of CHAP, both of which only express the CHAPa isoform, are present in the heart during embryonic development from the cardiac crescent stage onwards, but at later stages can be detected in somites and smooth muscle cells<sup>7</sup>. Morpholino-mediated knockdown of *chap* in the zebrafish resulted in impaired heart looping, cardiac oedema, decreased cardiac contractility and impaired skeletal muscle formation, demonstrating the importance of *chap* during muscle development<sup>6,7</sup>.

CHAP displays highest homology to myopodin and synaptopodin. Whilst synaptopodin is expressed in the brain and kidney, myopodin, like CHAP, is expressed in skeletal muscle, smooth muscle and heart<sup>8,9</sup>. Both synaptopodin and myopodin bind to  $\alpha$ -actinin and are involved in actin signalling. Synaptopodin induces filamentous actin (F-actin) formation via  $\alpha$ -actinin in an isoform dependent manner in neurons and kidney podocytes<sup>9</sup>. In podocytes, stress fiber formation by synaptopodin is regulated by preventing proteasomal breakdown of RhoA<sup>10</sup>. Myopodin on the other hand, is localized at the Z-disc through binding to  $\alpha$ -actinin; its phosphorylation leads to detachment from the Z-disc and subsequent translocation to the nucleus<sup>11</sup>, suggesting a role in molecular regulation by converting signaling pathways to downstream nuclear events.

Here, we demonstrate that CHAP initiates hypertrophic cardiomyopathy in transgenic mice if, specifically over-expressed in the heart. This was specific for CHAPb since the hearts of CHAPa Tg mice appeared normal up to one year of age. CHAPb Tg mice developed cardiac hypertrophy, fibrosis, left atrial enlargement as well as delayed atrial conduction, cardiac diastolic dysfunction and impaired calcium handling. Furthermore, activation of actin

signaling in these transgenic mice led to the formation of stress fibers. Together the results indicate that the fetal isoform CHAPb may be a novel candidate gene for cardiac hypertrophy and familial cardiomyopathies.

## Material and methods

### *Generation of CHAP Tg mice*

Full length cDNA of mouse CHAPa or b cDNA, preceded by a N-terminal Flag and Kozak consensus sequence, was fused to the heart-specific murine  $\alpha$ -myosin heavy chain ( $\alpha$ -MHC) promoter. At the 3' end of CHAP a poly-A-signal of the human growth hormone (hGH) was included. Plasmid DNA was linearized by digestion with NotI, gel purified and dialyzed against Tris-EDTA (TE) buffer. DNA was injected into pronuclei from mice with a C57BL/6-CBA background. Transgenic (Tg) founder mice were crossed back (5 generations) to C57BL/6 mice to obtain a pure background. For genotyping genomic DNA was isolated from mice tail biopsies and analysed by PCR with a forward primer recognizing the C-terminus of CHAP (5'-TGGTGAAACCCCGTCTCTAC-3') and a reverse primer recognizing the hGH polyA signal (5'-CAGATTTTCCACTCCTGCAC-3'). All animal experiments were performed according to the regulations of the Leiden University Medical Center.

### *Protein isolation and western blot analysis*

CHAP Tg mice and wild type littermates were sacrificed by cervical dislocation. Hearts were harvested, rinsed in PBS, snap frozen in liquid nitrogen and stored at  $-80^{\circ}\text{C}$  until further use. Hearts were homogenized using an ultra-turrax tissue separator (IKA, Germany) in T-PER tissue protein extraction reagent (Pierce) with extra added protein inhibitors (protease inhibitor cocktail tablets (10  $\mu\text{g}/\text{ml}$ ; Roche, Germany), 0.1 mmol/L dithiothreitol (DTT; Invitrogen) and 1 mmol/L phenylmethanesulfonylfluoride (PMSF; Sigma Aldrich), 5 mmol/L NaF and 1 mmol/L  $\text{Na}_3\text{VO}_4$ ). Samples were incubated on ice for 15 minutes and centrifuged at 10.000 RPM at  $4^{\circ}\text{C}$  for 10 minutes and supernatants were transferred to new tubes. Protein concentration was determined by the Bradford assay (BioRad) using bovine serum albumin as a standard. Proteins (50 $\mu\text{g}/\text{lane}$ ) were separated by SDS-page gel electrophoresis and subsequently blotted using Hybond-P membranes (GE Healthcare) 3 hours at RT. Incubation with the following antibodies was performed overnight at  $4^{\circ}\text{C}$  in 5% milk/TBS-Tween (unless stated else): CHAP (1:200, custom made by Eurogentec MW CHAPa=140 kDa, MW CHAPb=110 kDa), actin (1:1000; Millipore BV, MW=43 kDa), RhoA (1:200, 26C4, Santa Cruz, MW=24 kDa), alpha-actinin (1:800, EA-53, Sigma-Aldrich Chemie, MW=100 kDa), Ezrin/Moesin/Radixin (1:1000 in 5% BSA/TBS-Tween, Cell Signaling Technology MW moesin=75 kDa, MW Ezrin and Radixin=80 kDa), Cofilin (1:1000 in 5% BSA/TBS-Tween, Cell Signaling Technology, MW=19 kDa), SRF (1:200, G20, Santa Cruz, MW=40-67 kDa), Myocyte Enhancer Factor 2 (MEF2, 1:200, C21, Santa Cruz, MW=40-65 kDa) and GAPDH (1:10000, 6C5, Millipore, MW=38 kDa). Peroxidase-conjugated antibodies used were anti-mouse IgG HRP linked antibody (1:1000, Cell Signaling Technology) and anti-rabbit HRP linked antibody (1:2000, Cell Signaling Technology). For the detection of protein bands SuperSignal West Pico Chemiluminescent Substrate (Pierce) was (the substrate) used.

### *Southern blot analysis*

Genomic DNA of wild-type and CHAPb Tg mouse tails was extracted by adding 0.5 ml tail lysisbuffer (50 mM Tris pH 8.0, 100 mM EDTA pH 8.0, 100mM NaCl, 1% SDS and 10 mg/ml prot K) at  $55^{\circ}\text{C}$  overnight. DNA was precipitated by phenol-chloroform extraction and 10  $\mu\text{g}$  DNA was digested by adding BamHI (Promega) or XmnI (New England Biolabs) overnight and run on a 1% v/w agarose gel. Probes were generated using the following primers: 5'-

AGGGGTCCAGCTCTTTGAAC-3' and 5'-AGGCTTAAAGCGTCCTCCTC-3'. The PCR products were then radioactively labelled using  $\alpha$ -[p32]dATP (PerkinElmer) by random priming (RadPrime, Invitrogen). DNA blots (Hybond-N+, GE Healthcare) were hybridized with the radioactive probe in ExpressHyb Hybridization buffer (Clontech) and visualized by using a Phosphorimager.

#### RNA isolation and quantitative PCR

Transgenic and wild-type hearts were homogenized in TRIzol (Invitrogen) using an ultraturax tissue separator (IKA, Germany) and RNA was isolated according to the supplier's protocol. RNA was treated with DNase (DNA-free, Ambion) and cDNA was made with the iScript kit (BioRad). qPCR was performed using the CFX96 Real-Time PCR detection system (Bio-Rad). Primers used are listed in supplemental table 1. Data were analyzed with Bio-Rad CFX Manager.

Table 1: list of qPCR primers used

Gene name	Sequence	Melting temp. (°C)	Remarks
<i>ChapA</i>	5'-GAGGAGGTGCAGGTCACATT-3' 5'-CTGAAGAGCCTGGGAAACAG-3'	58	
<i>ChapB</i>	5'-CCGCCGCTTCTTAAACATAA-3' 5'-GGCTTTAAAGGGCCTTGG-3'	58	endogenous
<i>ChapB</i>	5'-CCAAGCCAGCTGTGACAAA-3' 5'-CCGCCGCTTCTTAAACATAA-3'	58	Endogenous + transgenic
<i>Connexin40</i>	5'-CTGGTCACTGTCCTGTTCA-3' 5'-GCAACCAGGCTGAATGGTAT-3'	60	
<i>Connexin43</i>	5'-TGGACAAGGTCCAAGCCTAC-3' 5'-ACAGCGAAAGGCAGACTGTT-3'	60	
<i>Connexin45</i>	5'-AAGAGCAGAGCCAACCAAAA-3' 5'-CCCACCTCAAACACAGTCCT-3'	60	
<i>CollagenI</i>	5'-GAGCGGAGAGTACTGGATCG-3' 5'-GTTCTGGGCTGATGTACCAGT-3'	60	
<i>CollagenIII</i>	5'-ACCAAAGGTGATGCTGGAC-3' 5'-GACCTCGTGCTCCAGTTAGC-3'	60	
<i>Nppa</i>	5'-GGGGTAGGATTGACAGGAT-3' 5'-CAGAATCGACTGCCTTTTCC-3'	60	
<i>Nppb</i>	5'-ACAAGATAGACCGGATCGGA-3' 5'-ACCCAGGCAGAGTCAGAAAC-3'	60	
<i>Myh7</i>	5'-GAGCCTGGATTCTCAAACG-3' 5'-CTTGCTACCCTCAGGTGGCT-3'	60	
<i>Serca2</i>	5'-TACTGACCCTGTCCCTGACC-3' 5'-CACCACCACTCCCATAGCTT-3'	60	
<i>GAPDH</i>	5'-GTTTGTGATGGGTGTGAACCAC-3' 5'-CTGGTCCTCAGTGTAGCCCAA-3'	58	Reference gene
<i>H2A</i>	5'-GTCGTGGCAAGCAAGGAG-3' 5'-GATCTCGGCCGTTAGGTACTC-3'	60	Reference gene
<i>PGK</i>	5'-TGAGAAAAGGAAGTGAGCTGTA-3' 5'-AGATTGCCATGCTGAGTC-3'	52	Reference gene

### *Transmission Electron Microscopy (TEM)*

Hearts of CHAPb Tg mice and wild type littermates were collected and left ventricles were used for TEM. Tissues were cut into smaller pieces (1 mm<sup>3</sup>). For electron microscopy samples were fixed in glutaraldehyde (2.5%) in 0.1 mol/L phosphate buffer for 24 hours, post fixed in 1% OsO<sub>4</sub> in 0.1 mol/L cacodylate buffer for 1 hour at 4°C, dehydrated in a graded ethanol series and embedded in an epoxy resin. Ultrathin sections were post stained with uranyl acetate and lead citrate and viewed and imaged with a FEI Tecnai 12 transmission electron microscope, operated at 120 kV and equipped with an Eagle 4kx4k camera (FEI, Eindhoven, The Netherlands)

### *Immunohistochemistry*

For histological and immunohistochemical analysis hearts were obtained at different time points (1, 3 and 6 months). Mice were sedated by injection of a mixture of 100 µl ketamine, 50 µl rompun and 10 µl atropine in 1ml 0.9% NaCl.

For paraffin sections mice were perfused with 0.9% NaCl and subsequently with 4% paraformaldehyde (PFA). Hearts and other organs (lungs, kidney and liver) were dissected, fixed over night in 4% PFA, dehydrated by ethanol-xylene series and embedded in paraffin. Serial heart sections (5 µm) were made, mounted on starfrost slides (Knittel) and followed by hematoxylin-eosin (HE) staining, Sirius red staining, and immunohistochemistry as indicated. For all antibody stainings, except Myosin Light Chain 2a (MLC2a), microwave antigen retrieval in citrate buffer (pH 6) was applied. Endogenous peroxidase was blocked by incubating the slides in 0.3% H<sub>2</sub>O<sub>2</sub> in PBS. Sections were incubated overnight at room temperature with Connexin40 antibody (1:100; Santa Cruz), Connexin43 (1:500; Zymed), MLC2a (1:4000 gift from S. Kubalak) and Troponin I (TnI, 1:800; Santa Cruz). Secondary antibody used was biotin-labeled goat anti-rabbit (Vector Labs) or biotin-labeled horse anti-goat (Vector Labs). Subsequently, the sections were incubated with Vectastain ABC staining kit (Vector Labs) for 45 min. Slides were rinsed in PBS and Tris/Maleate (pH 7.6). 3-3'-diaminobenzidine tetrahydrochloride (DAB, Sigma-Aldrich Chemie) was used as chromogen and Mayer's hematoxylin as counterstaining. Finally, slides were dehydrated and mounted with Entellan (Merck).

For cryosections mice were perfused with 0.9% NaCl only, then hearts were isolated. Processing of hearts for cryosections was adapted from Bajanca et al.<sup>12</sup>. In brief hearts were fixed in 0.2% PFA solution containing 4% sucrose, 0.12 mmol/L CaCl<sub>2</sub>·2H<sub>2</sub>O, 0.2 mol/L Na<sub>2</sub>HPO<sub>4</sub>·2H<sub>2</sub>O, 0.2 mol/L NaH<sub>2</sub>PO<sub>4</sub>·H<sub>2</sub>O over night at 4°C. Thereafter, hearts were washed in the same solution without PFA during the day at 4°C followed by a solution containing 0.24 mol/L phosphate buffer and 30% sucrose over night at 4°C. The next day hearts were embedded in Tissue-Tek (Sakura) on dry ice and stored at -20°C until sectioning. Serial sections (5 µm) were made and mounted on starfrost slides (Knittel) and antibody staining was performed as previously described<sup>13</sup>. Antibodies used were CHAP (1:50), myomesin (1:50 E. Elher), α-actinin (Sigma Aldrich), RhoA (1:100, 26C4, Santa Cruz) and pERM (1:50, Cell Signaling Technology). Secondary antibodies used are Cy-3 conjugated anti-mouse (1:250, Jackson ImmunoResearch Laboratories) and Alexa488 conjugated anti-rabbit (1:200, Invitrogen). Cell nuclei were counterstained with DAPI (Molecular Probes). Stainings were analyzed with SP5 confocal microscope (Leica).

### *Volume measurements*

The volume of the atria and ventricle was estimated by the Cavalieri principle. For this serial sections were stained for an atrial marker, MLC2a, or TnI to identify the ventricle. Then a grid was used to estimate the surface of the stained section and the distance between the sections was used to estimate the volume.

### *Magnetic Resonance Imaging (MRI)*

For MRI measurements 4 wild type and 5 CHAPb transgenic mice of 6 months of age were used. Animals were sedated by 4% isofluran and MRI images were produced as described below.

#### Hardware

All experiments were performed on a vertical 9.4T magnet (Bruker, Ettlingen, Germany) supplied with an actively shielded Micro2.5 gradient system of 1T/m and a 30 mm transmit/receive birdcage RF coil, using Para vision 4.0 software.

#### MRI protocols

##### *In vivo:*

At the start of each examination, several 2D FLASH scout images were recorded in the transverse and axial plane of the heart to determine the orientation of the heart

A modified FLASH sequence with a navigator echo (IntraAngio) was used for retrospective CINE MRI with the following parameters:

Short-axis (oriented roughly perpendicular to the septum) and long-axis (oriented through the apex and aortic valve) cardiac cine MRI images with the navigator positioned through the aortic arch were acquired with the following parameters: hermite-shaped RF pulse 1 ms; FA 10°; 200 averages, TR 68.1 ms; TE 1.86 ms; reconstruction of 18 cardiac frames; FOV 2.56\*2.56 cm<sup>2</sup>; matrix 192\*192; in-plane resolution 133 μm, slice thickness 1.0 mm; total acquisition time approximately 30 min.

Heart function was assessed using MASS for Mice 5.1 software package (Leiden, The Netherlands) by manual delineation of LV and RV borders.

Based on these segmented areas, LV and RV area, end-diastolic volume (EDV), end-systolic volume (ESV), LV stroke volume (SV), and LV ejection fraction were computed automatically.

### *Electrocardiogram (ECG) measurements*

ECG measurements on wild type and CHAPb Tg mice of 6 months of age were performed as described in Henkens et al.<sup>14</sup>. In brief animals were sedated by 4% isofluran and ECG measurements were recorded for at least one minute. The data were analysed with the program LEADS and heart rate, PR duration and P duration were calculated.

### *Sarcomere measurements*

Hearts of CHAPb Tg mice and wild type litter mates were isolated at different time points (1 month and 3 months) and snap frozen in liquid nitrogen. Single cardiomyocytes were obtained by grinding hearts in liquid nitrogen. Cardiomyocytes were defrosted in relaxing solution (pH 7.0; 1 mmol/L free Mg<sup>2+</sup>, 1, 145 mmol/L KCl, 2 mmol/L EGTA, 4 mmol/L ATP, 10 mmol/L imidazole). Then cardiomyocytes were treated with relaxing solution containing 1% Triton-x-100 for 5 minutes, to remove the membranes. Cardiomyocytes were washed twice in relaxing solution to remove Triton-X-100. Single cardiomyocytes were placed between a force

transducer and piezoelectric motor. Isometric force measurements were performed at 15°C and a sarcomere length, measured in relaxing solution, of 2.2  $\mu\text{m}$ . The calcium concentrations of relaxing and activation solution (pH 7.1) were  $10^{-3}$  and 30  $\mu\text{mol/L}$ , respectively. Solutions with intermediate free  $[\text{Ca}^{2+}]$  were obtained mixing relaxing and activation solution. The first control activation was performed at maximum  $[\text{Ca}^{2+}]$  and thereafter, the resting sarcomere length was set to 2.2  $\mu\text{m}$  again. The second control measurement was performed to calculate the maximum isometric tension (force divided by cross-sectional area). The next measurements (4-5) were performed in submaximal  $[\text{Ca}^{2+}]$ , followed by a control measurement. Force values obtained from submaximal  $[\text{Ca}^{2+}]$  were normalized to control values.

#### *Protein phosphorylation*

Protein phosphorylation of sarcomeric proteins was measured in hearts of CHAPb Tg and wild type litter mates at 3 months of age. A detailed description of the procedure can be found in R. Zaremba et al.<sup>15</sup>. Briefly, samples were separated by SDS-page gels. Subsequently, gels were stained by SYPRO Ruby stain or Pro-Q Diamond Phosphoprotein Stain.

#### *Statistical analysis*

Data were analysed with GraphPad Prism. All data are expressed as mean + the standard error of the mean (SEM). Statistical analysis was performed using Student's unpaired t-test.  $P < 0.05$  was considered to be statistically different.

## Results

### *Ectopic CHAP expression in transgenic mice*

Many genes expressed during heart development, but not in the adult, are re-expressed in cardiac pathology. We previously identified CHAP as such a developmentally regulated and functional cardiac gene and here investigated whether it also has a role in the adult heart. For this purpose we generated transgenic mice that expressed either the CHAPa or CHAPb isoform in the heart using a construct under control of the cardiac-specific  $\alpha$ -myosin heavy chain (MHC) promoter and proceeded by an N-terminal FLAG-tag (Figure 1A). DNA vector

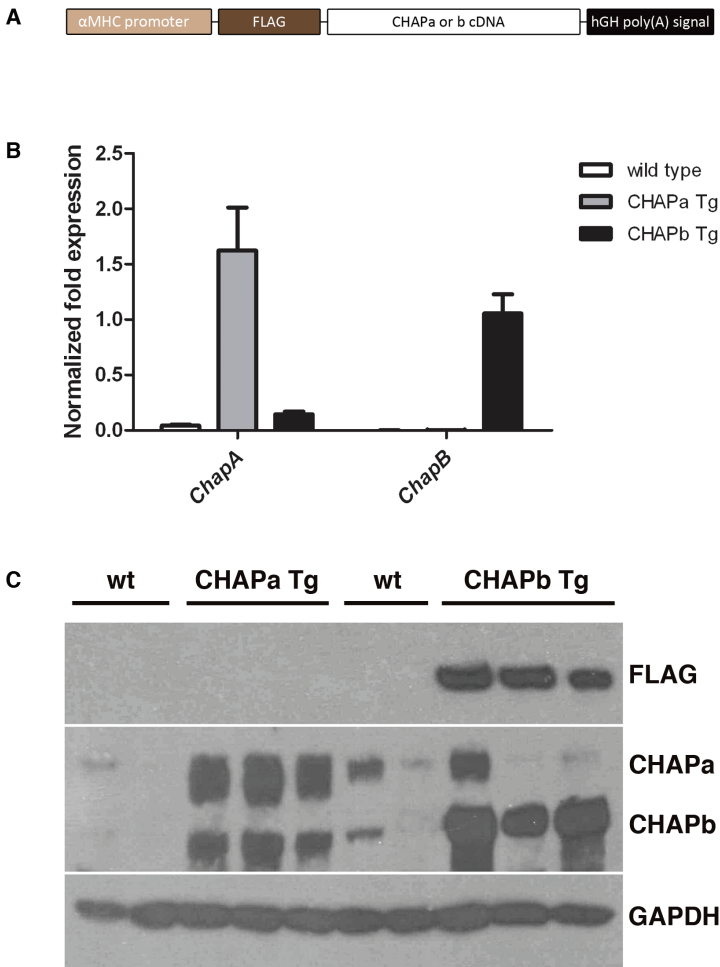


Figure 1: Expression analysis of CHAPa- and b Tg founders. A) Schematic overview showing the construct used to generate transgenic mice. FLAG-CHAPa- or b cDNA is downstream of the  $\alpha$ -MHC promoter and upstream a human Growth Hormone polyA signal. B) qPCR analysis of *ChapA* and *ChapB* in wt (white bars, n=6), CHAPa Tg (gray bars, n=4) and CHAPb Tg hearts (black bars, n=3). GAPDH was used as internal control. C) Western blot showing CHAP and flag expression in two wt and CHAPa Tg and two wt and CHAPb Tg hearts. GAPDH was used as loading control.

constructs were linearized and injected into C57BL/6-CBA zygotes. This resulted in two CHAPa transgenic (Tg) founders among 29 animals and three CHAPb Tg founders among 30 animals. First, we analysed the mRNA expression of *ChapA* and *ChapB* in the hearts of the offspring of the different transgenic lines. The two CHAPa Tg lines had comparable expression of *ChapA*. Analysis of *ChapA* mRNA in hearts of CHAPa Tg hearts by qPCR showed an expected upregulation (40-fold) compared to wild type (wt) mice (Figure 1B). Next, we analyzed the expression of CHAPa protein using an antibody that recognizes both CHAP isoforms. In wild type hearts, faint expression of CHAPa (140 kDa) was detected, whereas in CHAPa Tg mice strong expression of CHAPa could be detected. However, surprisingly, when using the anti-FLAG antibody no expression was observed. This could indicate that CHAPa was partially degraded or folded incorrectly at the site of the FLAG-epitope (Figure 1C). Histological analysis of CHAPa Tg hearts did not show any abnormalities at one and three months of age. Similarly, at one year of age no differences between wild type hearts and CHAPa Tg hearts was detected.

The three CHAPb Tg lines showed different copy number levels as determined by Southern blot (supplemental figure 1A). Analysis of hearts of the CHAPb Tg mouse line with intermediate copy numbers by qPCR demonstrated upregulation of *ChapB* compared to wt mice (Figure 1B). Western blot analysis of CHAPb Tg hearts showed a clear increase in CHAPb protein levels (110 kDa), when compared to wt hearts. This was confirmed by the presence of anti-FLAG immunoreactivity in the Tg hearts only (Figure 1C).

#### *Analysis of CHAPb Tg founder phenotype*

Southern blot analysis of founders showed high CHAPb copy number in transgenic line 29 and intermediate CHAPb copy number in line 14 compared to endogenous genomic levels of CHAP (supplemental figure 1A). CHAPb Tg founders died from around 6 months of age and onwards. The highest CHAPb expressing founder (CHAPb Tg line 29) died after 7 months, without progeny. Histological analysis of the heart of this founder is shown in supplemental figure 1B-D, left panels. Progeny of the CHAPb Tg line 14 died spontaneously at the earliest time point of approximately 6 months (supplemental figure 1B-D, right panels). Hearts of both transgenic lines (14 and 29) displayed comparable phenotypes with enlargement of left and right atrium (supplemental figure 1B,C). Histological analysis revealed that the left atrium was filled with a chronic and organized thrombus. Furthermore, thickness of the septum, left and right ventricle wall was increased, suggesting cardiac hypertrophy (supplemental figure 1B). This was confirmed by enlargement and apparent hypertrophy of cardiomyocytes on histological sections at higher magnifications (supplemental figure 1D).

#### *Overexpression of fetal isoform CHAPb in adult hearts leads to cardiac hypertrophy*

We analyzed CHAPb Tg mice at one, three and six months of age. At one month, heart of wt and CHAPb Tg mice were indistinguishable (supplemental figure 2A-C). At 3 months of age the left atrium of CHAPb Tg hearts was enlarged but without any signs of thrombus formation (figure 2A). Tg hearts showed obvious cardiomyocyte hypertrophy with enlarged nuclei (figure 2B) and interstitial fibrosis, as indicated by Sirius Red staining (figure 2C). To determine the extent of cardiac hypertrophy, we measured atrial and ventricular volume at one and three months of age. Myosin Light Chain 2a (MLC2a) and Troponin I (TnI) staining were used to identify the atria and ventricle, respectively. As expected, the myocardial volume of the left and right atrium at one month of age was similar in wt and CHAPb Tg mice

(supplemental figure 2D and E) but at 3 months, the left atrial volume of CHAPb Tg mice was significantly greater than in wt (wt  $2.046 \pm 0.1346$  n=4 mm<sup>3</sup>, CHAPb Tg  $4.598 \text{ mm}^3 \pm 0.3853$  n=4,  $p < 0.01$ ; figure 2E) although the volumes of the right atria were similar (wt  $2.041 \text{ mm}^3 \pm 0.2431$  n=4, CHAPb Tg  $2.114 \text{ mm}^3 \pm 0.03001$  n=4,  $p = \text{NS}$ ). Furthermore, despite the hypertrophy evident in individual cardiomyocytes of the left ventricle, the overall ventricular wall volume was not different in CHAPb Tg mice (wt  $57.81 \text{ mm}^3 \pm 6.352$  n=4, CHAPb Tg  $51.31 \text{ mm}^3 \pm 2.705$  n=4,  $p = \text{NS}$ ).

By 6 months of age, left atrial enlargement was consistently more pronounced in Tg mice and was associated with cardiomyocyte hypertrophy and interstitial fibrosis (Figure 2B, C). Occasionally, intraventricular thrombi were identified (Figure 2D). In general, changes in CHAPb Tg hearts were more pronounced at 6 months of age, displaying features that resemble cardiomyopathy, including sudden death.

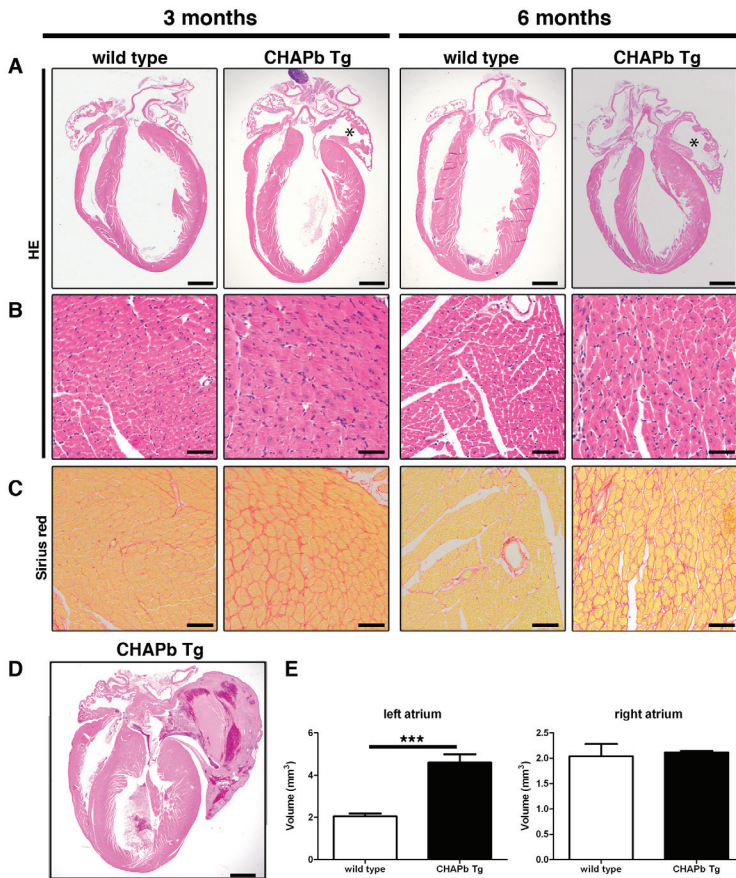


Figure 2: HE and Sirius red staining of CHAP Tg hearts. Wt (left panels) and CHAPb Tg (right panels) at 3 and 6 months of age (A-C). A) HE stained overview section. The left atrium in CHAPb Tg hearts is enlarged (indicated by \*) compared to wt litter mates. B) Higher magnification of left ventricle. In the left ventricle of CHAPb Tg hearts the cardiomyocytes are hypertrophic. C) Sirius red staining of the left ventricle showing increase in interstitial fibrosis in CHAPb Tg. D) CHAPb Tg heart with severe phenotype showing pronounced atrial enlargement, filled by a thrombus and thickening of the ventricles. E) Myocardial volume of the left atrium (left panels) and right atrium (right panels) in wt (white bars) and CHAPb Tg (black bars) hearts at 3 months of age. Scale bars 1 mm in A and D, 50  $\mu\text{m}$  in B, C.

### Activation of hypertrophic gene program and collagens in CHAPb Tg hearts

A hallmark of hypertrophy is re-expression of fetal cardiac genes, such as atrial natriuretic factor (ANF, *Nppa*), brain natriuretic peptide (BNP, *Nppb*) and  $\beta$ -MHC (*Myh7*). To investigate if the hypertrophy induced by CHAPb in Tg mice was also accompanied with upregulation of these genes, we isolated RNA from left ventricles of 6 month old wt (n=3) and CHAPb Tg (n=3) mice. qPCR analysis showed significant upregulation of *Nppa* (17.2x, p<0.01, Figure 3A), *Nppb* (3.6x, p<0.01, Figure 3B) and *Myh7* (28.3x, p= 0.0634, Figure 3C) in Tg hearts. Activation of the same genes was also evident in the right ventricle (data not shown). These findings corroborate the hypertrophic response observed morphologically.

Fibrosis is characterized by increased collagen production. To confirm Sirius red evidence, we analyzed the expression of *Collagen I* and *III*, the major fibrin forming collagen types, in the left ventricles of wt and CHAPb Tg mice. Increased expression of *Collagen I* (3.2x, p=0.0506, Figure 3D) and *III* (3.7x, p=0.0404, Figure 3E) was indeed observed in CHAPb Tg animals, as expected. Moreover, mRNA expression of *Serca2*, which encodes a protein involved in  $Ca^{2+}$  cycling<sup>16</sup> and is generally downregulated in cardiac hypertrophy, was also decreased in CHAPb Tg hearts (Figure 3F). Expression of hypertrophic genes and collagens was also increased in the right ventricle (data not shown).

Finally, we examined endogenous *Chap* isoforms in CHAPb Tg mice. *ChapA* mRNA expression was the same in wt and CHAPb Tg hearts (Figure 3G) and although endogenous *ChapB* appeared slightly increased, this was not statistically significant (Figure 3I). Exogenous *ChapB* (Figure 3H) was, as expected, strongly upregulated in CHAPb Tg hearts compared to wt.

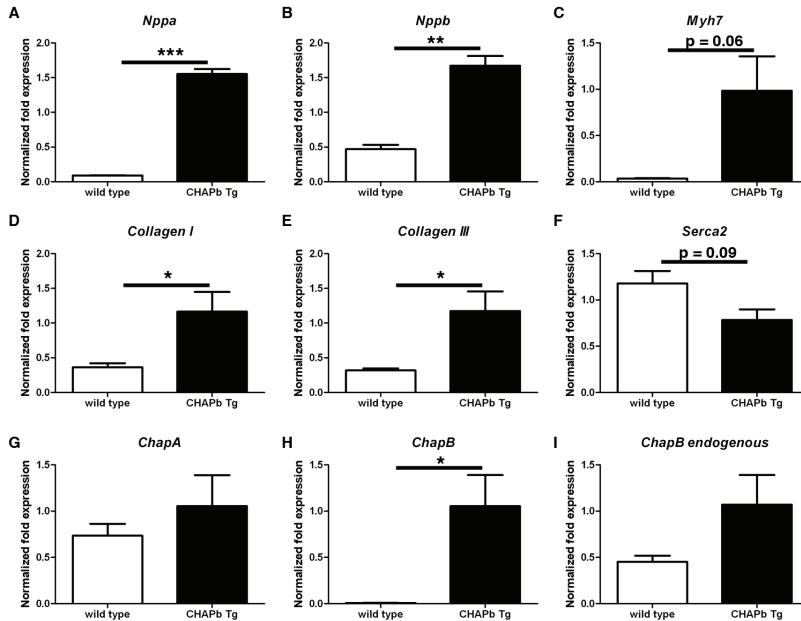


Figure 3: Expression of hypertrophy markers and collagens in left ventricle. qPCR analysis showing mRNA expression of *Nppa* (A), *Nppb* (B), *Myh7* (C), *CollagenI* (D), *CollagenIII* (E), *Serca2* (F), *ChapA* (G), *ChapB* (H) and endogenous *ChapB* (I) in the left ventricle of wt (white bars) and CHAPb Tg (black bars) mice. *GAPDH*, *PGK* and *H2A* were used as internal controls.

*Expression of CHAPb in adult heart leads to loss of Connexin expression in the left atria and conduction disturbances*

Since cardiomyopathies are associated with disturbed electrical conductance and cardiac arrhythmia, we investigated the most predominant Connexin (Cx) isoforms in atria and ventricles. Cx40 is the main isoform expressed in atria. Cx43 is expressed at higher levels in ventricles, although Cx43 is also expressed at low levels in the atria<sup>17</sup>. At one month of age, there was no difference in Cx40 and Cx43 expression between wt and CHAPb Tg (supplemental figure 3A and B). At three months, however, enlargement of the left atrium was accompanied by loss of expression of Cx's: both Cx40- and Cx43 immunoreactivity was reduced in the left atrium, although in the right atrium (supplemental figure 3C and D) and ventricles they were unchanged. This decrease in Cx40 and Cx43 levels in the left atrium was more pronounced at 6 months (figure 4A). These findings were confirmed by qPCR, which indeed showed that Cx40 (-23x,  $p < 0.01$ , figure 4B) and 43 (-6.9x,  $p < 0.01$ , supplemental figure 3E) were both downregulated in the left atrium. Similar to the protein data, mRNA expression of Cx40 and Cx43 in the right atrium was unchanged (Figure 4C and supplemental figure 3F). Expression of Cx45, which is specifically expressed in the sinoatrial- and atrioventricular nodes and is co-expressed with other isoforms in the rest of the conduction system<sup>17</sup>, was unchanged in the left atrium.

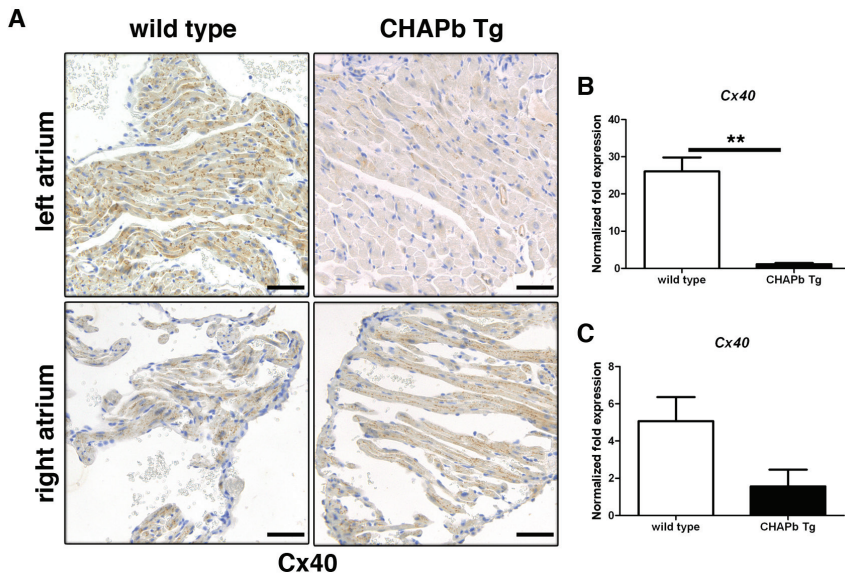


Figure 4: Decreased Connexin 40 expression in CHAPb Tg left atrium at 6 months of age. Immunohistochemical staining showing Connexin 40 (A) expression in wt (left panels) and CHAPb Tg (right panels) left (upper panels) and right (lower panels) atria. qPCR analysis of *Connexin 40* (B and C) expression in the left (B) and right (C) atrium. Scale bars 50  $\mu$ m.

To investigate whether the loss of expression of Cx40 and 43 was correlated with conduction disturbances, we performed ECG measurements of wt and CHAPb Tg mice. These measurements showed that the PR interval was increased in CHAPb Tg mice (wt 40,89 ms  $\pm$  1,150 n=3, CHAPb Tg 49,83  $\pm$  1,784 n=8,  $p < 0.05$ ; Figure 5A) indicating a conduction delay from atria to ventricles. No signs of atrial fibrillation were observed, as the duration of the P-top was not changed (wt 7,367 ms  $\pm$  0,9260 n=3, CHAPb Tg 6,955 ms  $\pm$  0,4934 n=8,  $p = ns$ ; Figure 5B)<sup>18</sup>.

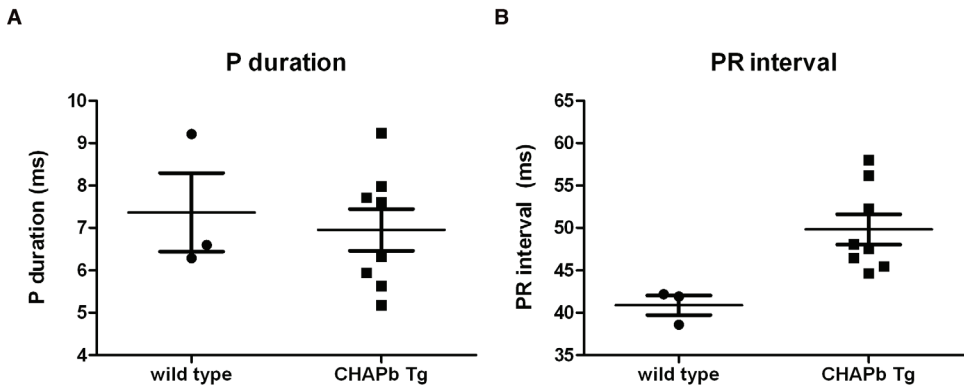


Figure 5: Conduction disturbances in CHAPb Tg mice at 6 months of age. ECG analysis of wt and CHAPb Tg mice showing PR interval (A) and P duration (B).

#### *CHAPb Tg mice show decreased cardiac performance*

To determine whether the phenotypic changes in CHAPb Tg hearts affected cardiac performance, we performed MRI measurements on 5 male wt and 5 male CHAPb Tg mice at 6 months of age. Enlargement of the left atrium was clearly visible in the scans. We then calculated the functional parameters of the left and right ventricle. The results of the left ventricle are shown in figure 6. Representative scans for wt and CHAPb Tg are shown in figure 6A. Both the end diastolic volume (wt  $45.81 \mu\text{l} \pm 2.297$  n=4, CHAPb Tg  $29.08 \mu\text{l} \pm 1.176$  n=5,  $p < 0.01$ ; Figure 6B) and end systolic volume (wt  $15.72 \mu\text{l} \pm 2.570$  n=4, CHAPb Tg  $7.474 \mu\text{l} \pm 1.702$  n=5,  $p < 0.05$ ; Figure 6C) were significantly decreased in the left ventricle, which resulted in the ejection fraction being similar in wt and CHAPb Tg mice (wt  $66.26 \% \pm 3.972$  n=4, CHAPb Tg  $74.35 \% \pm 5.376$  n=5,  $p = \text{ns}$ ; Figure 6D). However, the cardiac output was significantly decreased in CHAPb Tg mice compared to wt (wt  $1559 \mu\text{l}/\text{min} \pm 32.20$  n=4, CHAPb Tg  $1083 \mu\text{l}/\text{min} \pm 117.6$  n=5,  $p < 0.01$ ; Figure 6E). Both the left ventricular mass of end diastole (wt  $77.79 \text{ mg} \pm 2.572$  n=4, CHAPb Tg  $58.11 \text{ mg} \pm 5.399$  n=5,  $p < 0.05$ ; Figure 6F) and end systole (wt  $93.97 \pm 1.784$  n=4, CHAPb Tg  $71.39 \pm 5.127$  n=5,  $p < 0.01$ ; Figure 6G) were decreased in CHAPb Tg mice. Similar data were obtained for the right ventricle (supplemental figure 4). Overall, these data show that CHAPb expression impairs diastolic and systolic function in both the left and right ventricle compared to wt mice.

#### *CHAPb Tg mice display decreased force generating capacity of cardiac sarcomeres*

To investigate the functional properties of cardiac sarcomeres, we measured force development at different calcium concentration in membrane-permeabilized single cardiomyocytes (Figure 6H) from wt and CHAPb Tg sarcomeres at 1 month of age. At the highest calcium concentration ( $30 \mu\text{mol}/\text{L}$ ) force development was decreased in CHAPb Tg cardiomyocytes (wt  $50.40 \text{ kN}/\text{m}^2 \pm 4.911$  n=12, CHAPb Tg  $30.23 \text{ kN}/\text{m}^2 \pm 4.346$  n=11,  $p = 0,006$ ; figure 6I). Furthermore, sarcomere  $\text{Ca}^{2+}$ -sensitivity ( $p\text{Ca}_{50}$ , the calcium concentration at which half of the maximum force was generated) was also decreased in CHAPb Tg sarcomeres compared to wt (wt  $5.53 \pm 0.02$  n=12, CHAPb Tg  $5.45 \pm 0.02$  n=11,  $p = 0,0046$ ; figure 6J). The reduction in both maximal force and  $p\text{Ca}_{50}$  shows that the CHAPb sarcomeres have less force generating capacity compared to wt sarcomeres. The phosphorylation status of the sarcomeric proteins troponin I and T, myosin binding protein C and myosin light chain 2, remained unchanged

(data not shown). These results correlated with the lower cardiac output observed in CHAPb Tg mice compared to wt mice, where we found decreased diastolic function, indicating a stiffer heart.

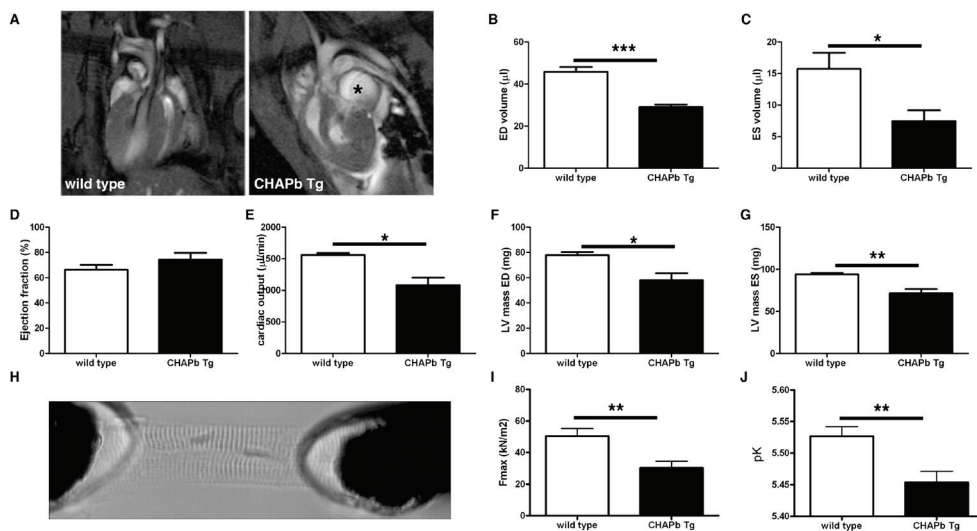


Figure 6: Functional analysis of CHAPb Tg hearts. A) Example images of wt and CHAPb Tg longitudinal sections. Enlarged LA in CHAPb Tg is indicated with \*. B-G) MRI measurements of the left ventricle of wt (white bars) and CHAPb Tg (black bars) animals at 6 months of age. ED volume (B), ES volume (C), ejection fraction (D), cardiac output (E), LV mass ED (F) and LV mass ES (G). H) Experimental setup for single membrane-permeabilized cardiomyocyte measurements to determine sarcomeric function. Sarcomeric force measurements at one month of age showed reductions in maximum force (I; Fmax) and  $\text{Ca}^{2+}$ -sensitivity (J;  $\text{pCa}_{50}$ ) in CHAPb Tg (black bars) compared to wt (white bars). ED (end diastolic), ES (end systolic) and LV (left ventricular).

#### *Sarcomeric organization is disturbed in CHAPb Tg hearts*

Next we investigated the sarcomeric organization in cryosections of wt and CHAPb Tg hearts. Immunohistochemical staining for CHAP,  $\alpha$ -actinin (Z-disc protein) and myomesin (M-band protein) showed that both CHAP and  $\alpha$ -actinin were co-localized at the Z-disc of cardiomyocytes in wt hearts (Figure 7A), whereas CHAP did not overlap with myomesin (supplemental figure 5). In CHAPb Tg hearts, CHAP was also localized at the Z-disc with  $\alpha$ -actinin (Figure 7A) and did not overlap with myomesin (supplemental figure 5). However, in the CHAPb Tg hearts, CHAP was also localized in fibers, which appeared to be perpendicular to the sarcomeres and resembled the formation of stress fibers. These fibers stained with  $\alpha$ -actinin (Figure 7A), but not myomesin (supplemental figure 5). The formation of these stress fibers was already visible at 1 month. To study this in more detail we performed Transmission Electron Microscopy on 6 months old wt and Tg hearts. In wt hearts the organization of the sarcomeres was regular with well-formed Z-discs and intercalated discs. In CHAPb Tg hearts the sarcomeres were clearly irregular and both Z-disc and intercalated discs were disorganized (Figure 7B). These data indicate that in CHAPb Tg hearts the organization of the Z-discs and intercalated discs are disturbed.

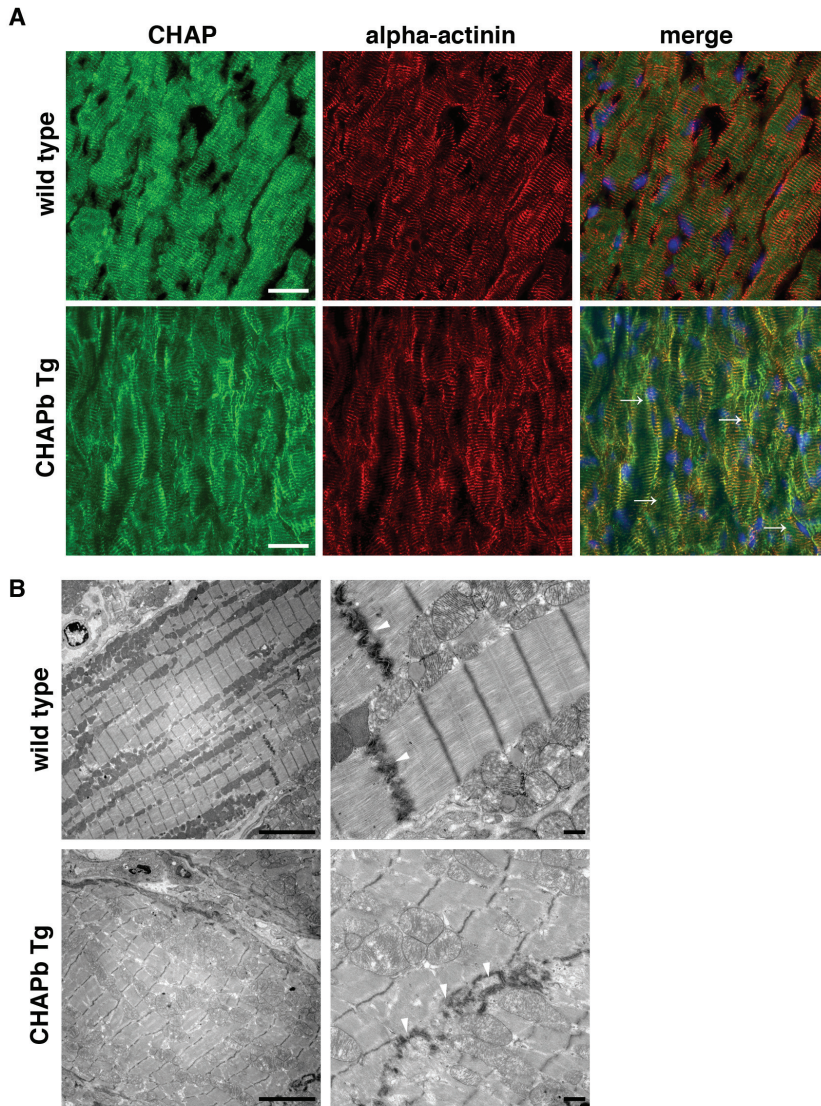


Figure 7: Sarcomeric organization is disturbed in CHAPb Tg hearts. Hearts stained for CHAP (green) /  $\alpha$ -actinin (red; A), merge images are shown. CHAP is localized in the Z-disc of cardiomyocytes of wt (upper panels) hearts. In cardiomyocytes of CHAPb Tg (lower panels) CHAP also stains stress fibers (arrows), which co-stain for  $\alpha$ -actinin. B) Electron microscopy analysis of wt and CHAPb Tg hearts at 6 months of age. In CHAPb Tg the sarcomeres were irregular and Z-discs and intercalated discs (arrow heads) are disorganized. Scale bars 20  $\mu$ m in A, 5  $\mu$ m in left panels and right panels 1  $\mu$ m of B.

#### *Activation of the actin signalling pathway in CHAPb Tg hearts*

Since synaptopodin, a CHAP family member, has been associated with actin signalling in other tissues such as brain and kidney and since the actin signalling pathway is also involved in cardiac hypertrophy, we investigated whether components of the actin signalling pathway were activated in CHAPb Tg hearts. Staining of GTPase RhoA, a key component of the actin signalling pathway, in hearts at 6 months of age showed sarcomeric expression pattern in wt

hearts, while in CHAPb Tg hearts RhoA expression was increased and, interestingly, was displaced from its sarcomeric localization in cardiomyocytes (Figure 8A). To further confirm the CHAPb dependent activation of actin signalling, we examined downstream effectors. Indeed, phosphorylation of Ezrin/radixin/moesin (ERM), a family of proteins involved in Rho-dependent signalling and linking the actin cytoskeleton to the plasma membrane<sup>19, 20</sup>, was increased in CHAPb Tg hearts and co-localized with CHAP (supplemental figure 6) and RhoA. Increased protein expression levels of RhoA, actin,  $\alpha$ -actinin, ERM, cofilin, and downstream actin-dependent transcription factors serum response factor (SRF) and myocyte enhancer factor-2 (MEF2) in hearts of CHAPb Tg compared to wt (figure 8B) confirmed these findings. These results suggested CHAPb dependent activation of the actin-signalling pathway, from membrane to the nucleus, which may contribute to the molecular, phenotypic and functional alterations observed in the transgenic mice.

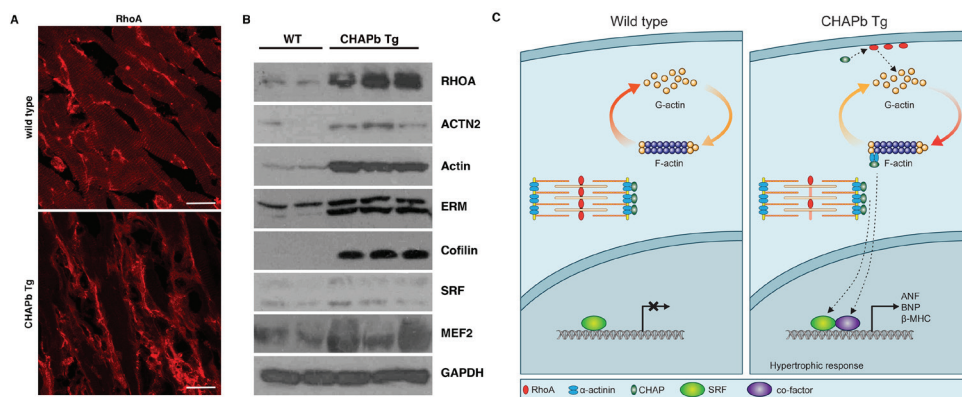


Figure 8: Increased actin signaling in CHAPb Tg hearts. A) Wt (upper panels) and CHAPb Tg (lower panels) hearts at 6 months of age stained for RhoA (red). In wt mice RhoA is localized at the membrane of cardiomyocytes and shows a sarcomeric expression pattern. In CHAPb Tg hearts sarcomeric expression of RhoA is decreased and membrane expression is increased. B) Western blot analysis of 2 wt and 3 CHAPb Tg hearts at 6 months of age for RhoA,  $\alpha$ -actinin, actin, Ezrin (80 kDa)/moesin (80 kDa)/radixin (75 kDa; ERM), cofilin, SRF (40 – 67kDa) and MEF2. GAPDH is used as loading control. C) Summarizing model: in wt mice CHAPa is localized at the Z-disc with  $\alpha$ -actinin and there is no expression of CHAPb, leading to high G-actin expression resulting in low expression of SRF target genes. In CHAPb Tg mice CHAPb expression results in activation of RhoA, leading to a shift from G-actin to F-actin, binding of co-factors to SRF and activation of SRF target genes, such as ANF, BNP and  $\beta$ -MHC. In addition signaling of CHAPb to SRF might also be directly through binding of CHAPb and  $\alpha$ -actinin to F-actin fibers or through the Z-disc. Scale bars: 20  $\mu$ m.

## Discussion

Here we show for the first time that the Z-disc protein CHAP can initiate cardiac disease. CHAP was initially identified as a gene upregulated during the differentiation of human embryonic stem cell-derived to cardiomyocytes<sup>5</sup>. In mice and human two CHAP splice variants were identified which differ in their temporal expression patterns: the shorter isoform CHAPb is expressed during embryonic development in the heart, somites and muscle precursors, whilst CHAPa is expressed in the adult heart and skeletal muscle. Morpholino knockdown of *Chap* in zebrafish showed that it is essential for heart development. Furthermore, overexpression of “embryonic” CHAPb, but not “adult” CHAPa, in rat cardiomyocytes led to dissociation of  $\alpha$ -actinin-2 from the Z-disc<sup>6</sup>. In agreement with these findings, we found that overexpression of CHAPa in the adult mouse heart had no effect on cardiac morphology or function, whilst CHAPb Tg mice displayed features which are comparable to cardiomyopathy, such as cardiac hypertrophy, interstitial fibrosis, diastolic dysfunction, and disturbed electrical conductance, which led to higher mortality.

### *CHAPb induces cardiac hypertrophy, left atrial enlargement and fibrosis*

CHAPb overexpression in transgenic hearts was apparent both in qPCR and Western blot analysis. This had no effect at one month of age but by 3 months, molecular and cellular hypertrophy without ventricular wall thickening, left atrial enlargement and interstitial fibrosis were clearly evident. This was more pronounced at 6 months of age and by then was occasionally accompanied by wall thickening of the left and right ventricles and septum. In agreement with increasing severity of the phenotype, CHAPb Tg mice died spontaneously from 6 months of age and onwards. Occasionally thrombi were found in the left atria, which may have disturbed blood flow in the left atrium and impaired ventricular filling. Reduced ventricular filling may eventually contribute to pulmonary venous congestion and development of pulmonary oedema. Although we did not observe pulmonary oedema overall (indicated by preserved lung weights) in CHAPb Tg mice, we cannot exclude that this occurred in individual mice. Indeed, occasionally MRI, revealed white/grey areas in lungs of CHAPb Tg mice, suggesting fluid retention.

### *Impaired structural and electrical organization at intercalated discs in CHAPb Tg hearts*

In addition to the morphological and histological changes in CHAPb Tg heart, we also observed changes at the intercalated discs of cardiomyocytes. In particular, gap junction proteins Cx40 and Cx43 were clearly downregulated in the left atrium of CHAPb Tg hearts, which was already visible at 3 months of age but more pronounced at 6 months. Since gap junctions are crucial for fast spreading of action potentials between cardiomyocytes, impaired expression of gap junctions would be expected to affect electrical guidance. Indeed, decreased connexins expression in the left atrium correlated with conduction disturbances, evidenced by increased PR interval, the time required for conduction between atria and ventricles. Loss of expression of Cx40 and 43 has been associated previously with conduction disturbances in mice. In Cx40<sup>-/-</sup> mutant mice, various conduction disturbances have been reported, including increased PR interval<sup>21, 22</sup>. In Cx43<sup>+/-</sup> mice ventricular conduction was delayed<sup>23</sup>, although no change in atrial conduction was observed<sup>24</sup>. In other hypertrophy mouse models, downregulation of Cx's in the atria also correlated with conduction disturbances<sup>25-27</sup>. Although decreased expression of connexins and impaired electrical guidance in CHAP

Tg mice was limited to the atria, detailed analysis of individual cardiomyocytes by electronmicroscopy showed that there was disorganization of Z-discs and intercalated discs throughout the whole heart. Sarcomeric disorganization would suggest impaired contractility and/or relaxation of cardiac muscle, affecting cardiac function.

#### *CHAPb Tg mice display cardiac diastolic dysfunction*

MRI measurements indicated that CHAPb Tg mice had normal left ventricular ejection fraction. Similarly, in patients with heart failure, almost half (47%) still have a normal ejection fraction<sup>28</sup>. Ejection fraction is determined by differences in both end diastolic and end systolic volumes and if both parameters are changed, as occurs in CHAPb Tg mice, ejection fraction may be unaffected. The decreased diastolic volumes observed in CHAPb Tg mice may suggest impaired relaxation during diastole (diastolic dysfunction), which relates to impaired  $\text{Ca}^{2+}$  cycling in cardiomyocytes. Contraction of cardiomyocytes is achieved by entry of  $\text{Ca}^{2+}$  through L-type channels, which causes  $\text{Ca}^{2+}$  release into the cytosol, immediately followed by  $\text{Ca}^{2+}$  release from the sarcoplasmic reticulum (SR). Subsequently,  $\text{Ca}^{2+}$  binds to sarcomeric protein troponin C to initiate contraction. On the other hand, relaxation occurs through uptake of the  $\text{Ca}^{2+}$  into the SR via SERCA2. In CHAPb Tg cardiomyocytes, re-uptake of  $\text{Ca}^{2+}$  might be affected, due to reduced levels of SERCA2<sup>16, 29</sup>. Indeed, we found that SERCA2 mRNA expression is reduced in the hearts of CHAPb Tg. In addition, measurements in membrane-permeabilized cardiomyocytes revealed reduced force generating capacity of CHAPb Tg sarcomeres, which may in part underlie the significant reduction in cardiac output observed in CHAPb Tg compared to wt mice. In primary cardiomyopathy, alterations in  $\text{Ca}^{2+}$ -sensitivity have been reported, which may depend on the location of the mutation in affected genes. Perturbations in  $\text{Ca}^{2+}$ -sensitivity of the sarcomeres may result in development of HCM or DCM<sup>30</sup>. As overexpression of CHAPb reduced  $\text{Ca}^{2+}$ -sensitivity, it would be interesting to investigate the role of CHAP in primary cardiomyopathy cases.

#### *Activated actin signalling in CHAPb Tg hearts*

We found that expression of RhoA is increased in CHAPb Tg hearts. RhoA belongs to the family of the small GTPases. Its effects on the actin cytoskeleton are mediated through stimulation of Rho Kinase (ROCK)<sup>31</sup>. RhoA is expressed in the heart during embryonic development, is downregulated after birth and re-expressed in cardiac hypertrophy<sup>32</sup>. Furthermore, RhoA transgenic mice develop a phenotype that resembles dilated cardiomyopathy (DCM), which is accompanied with conduction disturbances<sup>33</sup>. Alternatively, inhibition of ROCK reduces pressure overload-induced hypertrophy in rats<sup>34</sup>. It has been previously shown that synaptopodin, which has significant homology to CHAP, is involved in actin stress fiber formation by preventing proteasomal degradation of RhoA<sup>10</sup>. Like synaptopodin, CHAPb might be involved in the stabilization of RhoA, which may lead to actin stress fiber formation and induction of hypertrophy via the Rho-ROCK pathway.

#### *CHAP is involved in the SRF/MEF-2 actin signalling pathway*

We observed increased expression of transcription factors SRF and MEF-2 in CHAPb Tg hearts. Previously, it has been demonstrated that Striated muscle activator of Rho signaling (STARS), an actin-bundling protein that is localized at the Z-disc, is associated with both SRF and MEF-2 signalling. STARS is induced by MEF-2, which in turn regulates the formation of F-actin fibers via RhoA, leading to depletion of the monomeric globular

actin (G-actin) pool. Consequently, a reduction of G-actin may lead to activation of SRF mediated transcription<sup>35-37</sup>. Previous studies in mice have indicated the relevance of SRF in the development of cardiomyopathy<sup>38, 39</sup>. In addition, the importance of SRF in cardiomyocyte function, maintenance and regulation was shown in experiments in which it was knocked-down: expression of cytoskeletal genes, such as  $\alpha$ - and  $\beta$ -MHC, cardiac  $\alpha$ -actin and smooth muscle actin were decreased and also, interestingly, CHAP<sup>40, 41</sup>. With respect to the MEF2 transcription factor family (MEF-2a,c and d), Tg mice overexpressing these genes in the heart also showed cardiac hypertrophy and stress-dependent cardiac remodelling<sup>42-44</sup>. The phenotypes of the different Tg models do not overlap completely with the phenotype observed here, suggesting that additional pathways may be involved in the CHAPb induced hypertrophy. In summary, our study suggests a model in which increased levels of CHAPb may activate actin signalling leading to subsequent activation of cardiac transcription factors MEF2 and SRF, initiating a hypertrophic response and structural and functional changes in cardiomyocytes (figure 8C).

### Conclusion

We show that overexpression of the “embryonic” isoform of CHAP, CHAPb, in mice causes cardiomyopathy with diastolic cardiac dysfunction and conduction disturbances, which is associated with sarcomere dysfunction and activation of actin signalling and of the downstream transcription factors MEF-2 and SRF. In contrast, overexpression of “adult” isoform CHAP did not lead to cardiac phenotypical and functional changes. Recently, Kong<sup>45</sup> *et al* demonstrated that apart from alterations in gene expression, changes in mRNA splicing of sarcomeric genes particularly are associated with heart failure. These findings and our study demonstrate the importance of correctly spliced sarcomeric genes and substantiates further investigation in developmentally (dys-) regulated alternative splicing of other cardiac genes.

Taken together our results identify CHAPb as a novel component in the pathology of cardiomyopathy and a potential new candidate gene for screening mutations in familial cardiomyopathies.

## Acknowledgements

We thank L. Wisse, J. Korving, A.M. Mommaas-Kienhuis for technical assistance. We would like to thank Bas Blankevoort for graphics.

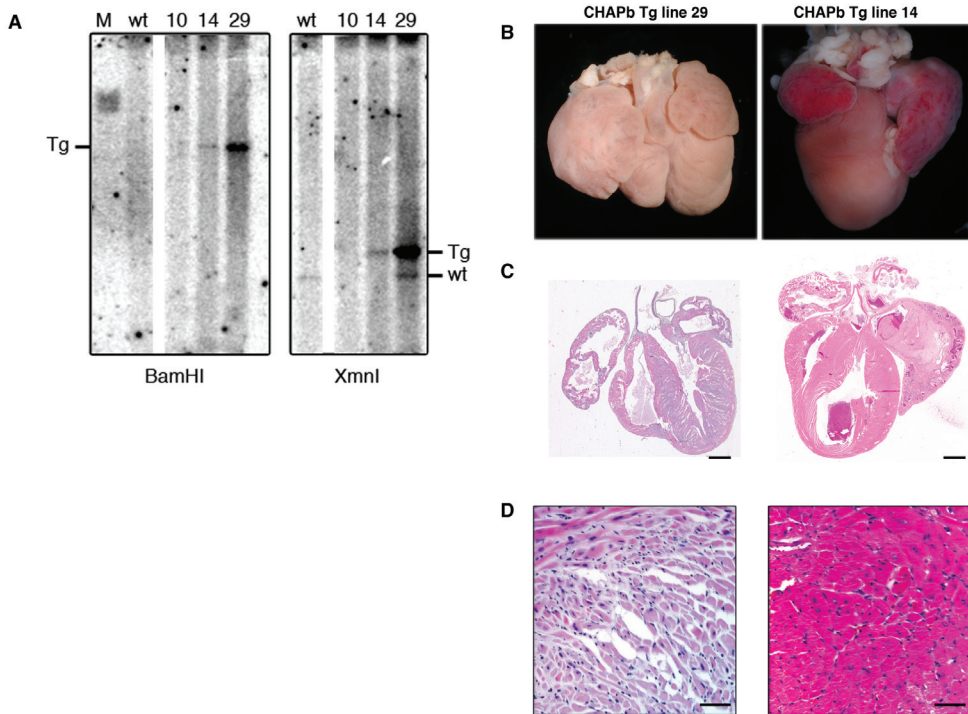
## References

- (1) Barry SP, Davidson SM, Townsend PA. Molecular regulation of cardiac hypertrophy. *Int J Biochem Cell Biol* 2008;40(10):2023-39.
- (2) Wilkins BJ, Molkentin JD. Calcium-calcineurin signaling in the regulation of cardiac hypertrophy. *Biochem Biophys Res Commun* 2004 October 1;322(4):1178-91.
- (3) Rohini A, Agrawal N, Koyani CN, Singh R. Molecular targets and regulators of cardiac hypertrophy. *Pharmacol Res* 2010 April;61(4):269-80.
- (4) Sanoudou D, Vafiadaki E, Arvanitis DA, Kranias E, Kontrogianni-Konstantopoulos A. Array lessons from the heart: focus on the genome and transcriptome of cardiomyopathies. *Physiol Genomics* 2005 April 14;21(2):131-43.
- (5) Beqqali A, Kloots J, Ward-van Oostwaard D, Mummery C, Passier R. Genome-wide transcriptional profiling of human embryonic stem cells differentiating to cardiomyocytes. *Stem Cells* 2006 August;24(8):1956-67.
- (6) Beqqali A, Monshouwer-Kloots J, Monteiro R, Welling M, Bakkers J, Ehler E, Verkleij A, Mummery C, Passier R. CHAP is a newly identified Z-disc protein essential for heart and skeletal muscle function. *J Cell Sci* 2010 April 1;123(Pt 7):1141-50.
- (7) van Eldik W, Beqqali A, Monshouwer-Kloots J, Mummery C, Passier R. Cytoskeletal heart-enriched actin-associated protein (CHAP) is expressed in striated and smooth muscle cells in chick and mouse during embryonic and adult stages. *Int J Dev Biol* 2011;55(6):649-55.
- (8) Weins A, Schwarz K, Faul C, Barisoni L, Linke WA, Mundel P. Differentiation- and stress-dependent nuclear cytoplasmic redistribution of myopodin, a novel actin-bundling protein. *J Cell Biol* 2001 October 29;155(3):393-404.
- (9) Asanuma K, Kim K, Oh J, Giardino L, Chabanis S, Faul C, Reiser J, Mundel P. Synaptopodin regulates the actin-bundling activity of alpha-actinin in an isoform-specific manner. *J Clin Invest* 2005 May;115(5):1188-98.
- (10) Asanuma K, Yanagida-Asanuma E, Faul C, Tomino Y, Kim K, Mundel P. Synaptopodin orchestrates actin organization and cell motility via regulation of RhoA signalling. *Nat Cell Biol* 2006 May;8(5):485-91.
- (11) Faul C, Dhume A, Schecter AD, Mundel P. Protein kinase A, Ca<sup>2+</sup>/calmodulin-dependent kinase II, and calcineurin regulate the intracellular trafficking of myopodin between the Z-disc and the nucleus of cardiac myocytes. *Mol Cell Biol* 2007 December;27(23):8215-27.
- (12) Bajanca F, Luz M, Duxson MJ, Thorsteinsdottir S. Integrins in the mouse myotome: developmental changes and differences between the epaxial and hypaxial lineage. *Dev Dyn* 2004 October;231(2):402-15.
- (13) van Laake LW, Passier R, Monshouwer-Kloots J, Nederhoff MG, Ward-van Oostwaard D, Field LJ, van Echteld CJ, Doevendans PA, Mummery CL. Monitoring of cell therapy and assessment of cardiac function using magnetic resonance imaging in a mouse model of myocardial infarction. *Nat Protoc* 2007;2(10):2551-67.
- (14) Henkens IR, Mouchaers KT, Vliegen HW, van der Laarse WJ, Swenne CA, Maan AC, Draisma HH, Schalij I, van der Wall EE, Schalij MJ, Vonk-Noordegraaf A. Early changes in rat hearts with developing pulmonary arterial hypertension can be detected with three-dimensional electrocardiography. *Am J Physiol Heart Circ Physiol* 2007 August;293(2):H1300-H1307.
- (15) Zarembo R, Merkus D, Hamdani N, Lamers JM, Paulus WJ, Dos RC, Duncker DJ, Stienen GJ, van der Velden J. Quantitative analysis of myofilament protein phosphorylation in small cardiac biopsies. *Proteomics Clin Appl* 2007 October;1(10):1285-90.
- (16) van der Velden J. Diastolic myofilament dysfunction in the failing human heart. *Pflugers Arch* 2011 April 13.
- (17) Severs NJ, Bruce AF, Dupont E, Rothery S. Remodelling of gap junctions and connexin expression in diseased myocardium. *Cardiovasc Res* 2008 October 1;80(1):9-19.
- (18) Perez MV, Dewey FE, Marcus R, Ashley EA, Al-Ahmad AA, Wang PJ, Froelicher VF. Electrocardiographic predictors of atrial fibrillation. *Am Heart J* 2009 October;158(4):622-8.
- (19) Louvet-Vallee S. ERM proteins: from cellular architecture to cell signaling. *Biol Cell* 2000 August;92(5):305-16.
- (20) Lee JH, Katakai T, Hara T, Gonda H, Sugai M, Shimizu A. Roles of p-ERM and Rho-ROCK signaling in lymphocyte polarity and uropod formation. *J Cell Biol* 2004 October 25;167(2):327-37.
- (21) Bevilacqua LM, Simon AM, Maguire CT, Gehrman J, Wakimoto H, Paul DL, Berul CI. A targeted

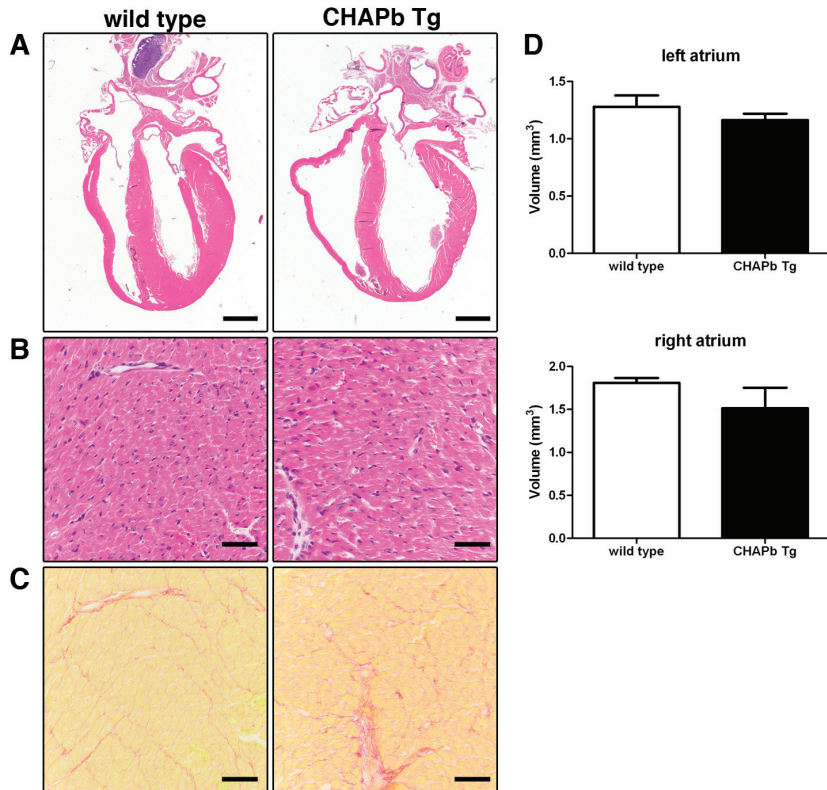
- disruption in connexin40 leads to distinct atrioventricular conduction defects. *J Interv Card Electrophysiol* 2000 October;4(3):459-67.
- (22) Kirchhoff S, Nelles E, Hagedorff A, Kruger O, Traub O, Willecke K. Reduced cardiac conduction velocity and predisposition to arrhythmias in connexin40-deficient mice. *Curr Biol* 1998 February 26;8(5):299-302.
- (23) Guerrero PA, Schuessler RB, Davis LM, Beyer EC, Johnson CM, Yamada KA, Saffitz JE. Slow ventricular conduction in mice heterozygous for a connexin43 null mutation. *J Clin Invest* 1997 April 15;99(8):1991-8.
- (24) Thomas SA, Schuessler RB, Berul CI, Beardslee MA, Beyer EC, Mendelsohn ME, Saffitz JE. Disparate effects of deficient expression of connexin43 on atrial and ventricular conduction: evidence for chamber-specific molecular determinants of conduction. *Circulation* 1998 February 24;97(7):686-91.
- (25) Wei L, Taffet GE, Khoury DS, Bo J, Li Y, Yatani A, Delaughter MC, Kleivitsky R, Hewett TE, Robbins J, Michael LH, Schneider MD, Entman ML, Schwartz RJ. Disruption of Rho signaling results in progressive atrioventricular conduction defects while ventricular function remains preserved. *FASEB J* 2004 May;18(7):857-9.
- (26) Ikeda Y, Sato K, Pimentel DR, Sam F, Shaw RJ, Dyck JR, Walsh K. Cardiac-specific deletion of LKB1 leads to hypertrophy and dysfunction. *J Biol Chem* 2009 December 18;284(51):35839-49.
- (27) Bierhuizen MF, Boulaksil M, van SL, van der Nagel R, Jansen AT, Mutsaers NA, Yildirim C, van Veen TA, De Windt LJ, Vos MA, van Rijen HV. In calcineurin-induced cardiac hypertrophy expression of Nav1.5, Cx40 and Cx43 is reduced by different mechanisms. *J Mol Cell Cardiol* 2008 September;45(3):373-84.
- (28) Owan TE, Hodge DO, Herges RM, Jacobsen SJ, Roger VL, Redfield MM. Trends in prevalence and outcome of heart failure with preserved ejection fraction. *N Engl J Med* 2006 July 20;355(3):251-9.
- (29) Kindermann M, Reil JC, Pieske B, van Veldhuisen DJ, Bohm M. Heart failure with normal left ventricular ejection fraction: what is the evidence? *Trends Cardiovasc Med* 2008 November;18(8):280-92.
- (30) Robinson P, Griffiths PJ, Watkins H, Redwood CS. Dilated and hypertrophic cardiomyopathy mutations in troponin and alpha-tropomyosin have opposing effects on the calcium affinity of cardiac thin filaments. *Circ Res* 2007 December 7;101(12):1266-73.
- (31) Brown JH, Del Re DP, Sussman MA. The Rac and Rho hall of fame: a decade of hypertrophic signaling hits. *Circ Res* 2006 March 31;98(6):730-42.
- (32) Ahuja P, Perriard E, Pedrazzini T, Satoh S, Perriard JC, Ehler E. Re-expression of proteins involved in cytokinesis during cardiac hypertrophy. *Exp Cell Res* 2007 April 1;313(6):1270-83.
- (33) Sah VP, Minamisawa S, Tam SP, Wu TH, Dorn GW, Ross J, Jr., Chien KR, Brown JH. Cardiac-specific overexpression of RhoA results in sinus and atrioventricular nodal dysfunction and contractile failure. *J Clin Invest* 1999 June;103(12):1627-34.
- (34) Phrommintikul A, Tran L, Kompa A, Wang B, Adrahtas A, Cantwell D, Kelly DJ, Krum H. Effects of a Rho kinase inhibitor on pressure overload induced cardiac hypertrophy and associated diastolic dysfunction. *Am J Physiol Heart Circ Physiol* 2008 April;294(4):H1804-H1814.
- (35) Kuwahara K, Teg Pipes GC, McAnally J, Richardson JA, Hill JA, Bassel-Duby R, Olson EN. Modulation of adverse cardiac remodeling by STARS, a mediator of MEF2 signaling and SRF activity. *J Clin Invest* 2007 May;117(5):1324-34.
- (36) Arai A, Spencer JA, Olson EN. STARS, a striated muscle activator of Rho signaling and serum response factor-dependent transcription. *J Biol Chem* 2002 July 5;277(27):24453-9.
- (37) Kuwahara K, Barrientos T, Pipes GC, Li S, Olson EN. Muscle-specific signaling mechanism that links actin dynamics to serum response factor. *Mol Cell Biol* 2005 April;25(8):3173-81.
- (38) Parlakian A, Charvet C, Escoubet B, Mericskay M, Molkentin JD, Gary-Bobo G, De Windt LJ, Ludovisky MA, Paulin D, Daegelen D, Tuil D, Li Z. Temporally controlled onset of dilated cardiomyopathy through disruption of the SRF gene in adult heart. *Circulation* 2005 November 8;112(19):2930-9.
- (39) Zhang X, Chai J, Azhar G, Sheridan P, Borrás AM, Furr MC, Khrapko K, Lawitts J, Misra RP, Wei JY. Early postnatal cardiac changes and premature death in transgenic mice overexpressing a mutant form of serum response factor. *J Biol Chem* 2001 October 26;276(43):40033-40.
- (40) Balza RO, Jr., Misra RP. Role of the serum response factor in regulating contractile apparatus gene expression and sarcomeric integrity in cardiomyocytes. *J Biol Chem* 2006 March 10;281(10):6498-510.
- (41) Miano JM, Ramanan N, Georger MA, de Mesy Bentley KL, Emerson RL, Balza RO, Jr., Xiao Q, Weiler H, Ginty DD, Misra RP. Restricted inactivation of serum response factor to the cardiovascular system. *Proc Natl Acad Sci U S A* 2004 December 7;101(49):17132-7.

- (42) van Oort RJ, van RE, Bourajjaj M, Schimmel J, Jansen MA, van der NR, Doevendans PA, Schneider MD, van Echteld CJ, De Windt LJ. MEF2 activates a genetic program promoting chamber dilation and contractile dysfunction in calcineurin-induced heart failure. *Circulation* 2006 July 25;114(4):298-308.
- (43) Kim Y, Phan D, van RE, Wang DZ, McAnally J, Qi X, Richardson JA, Hill JA, Bassel-Duby R, Olson EN. The MEF2D transcription factor mediates stress-dependent cardiac remodeling in mice. *J Clin Invest* 2008 January;118(1):124-32.
- (44) Xu J, Gong NL, Bodi I, Aronow BJ, Backx PH, Molkentin JD. Myocyte enhancer factors 2A and 2C induce dilated cardiomyopathy in transgenic mice. *J Biol Chem* 2006 April 7;281(14):9152-62.
- (45) Kong SW, Hu YW, Ho JW, Ikeda S, Polster S, John R, Hall JL, Bisping E, Pieske B, dos Remedios CG, Pu WT. Heart failure-associated changes in RNA splicing of sarcomere genes. *Circ Cardiovasc Genet*. 2010 Apr;3(2):138-46.

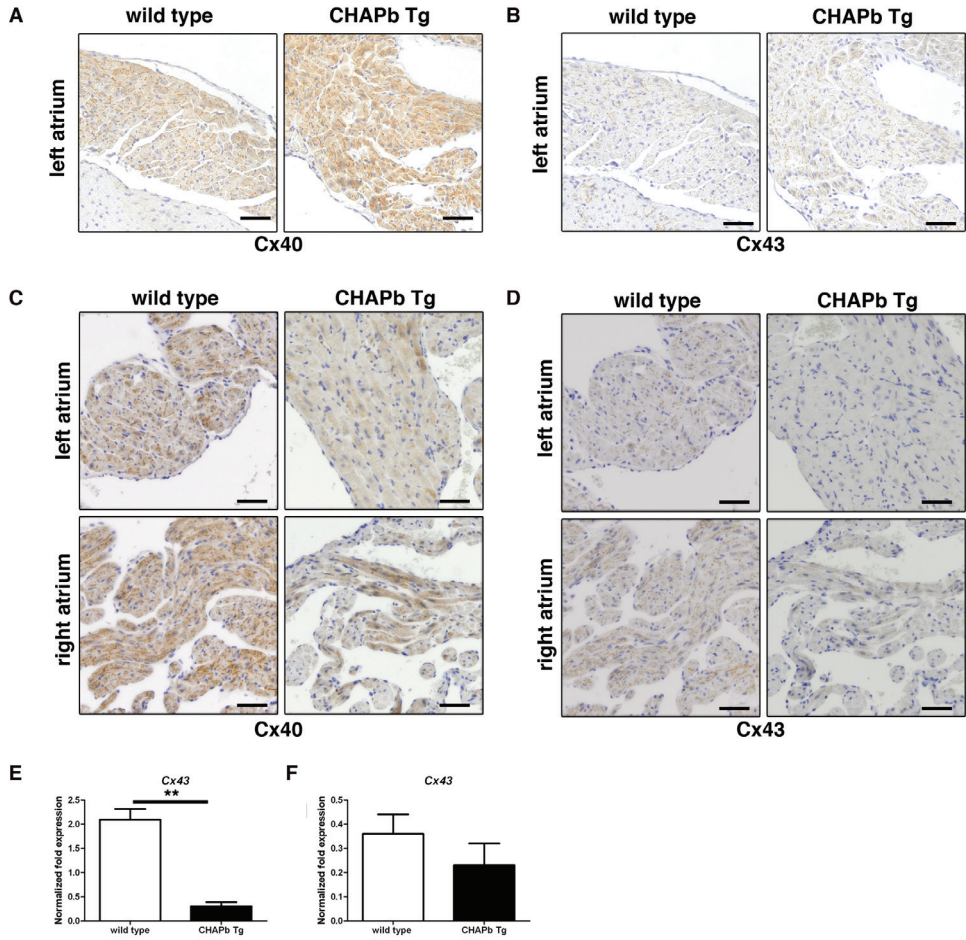
## Supplemental figures



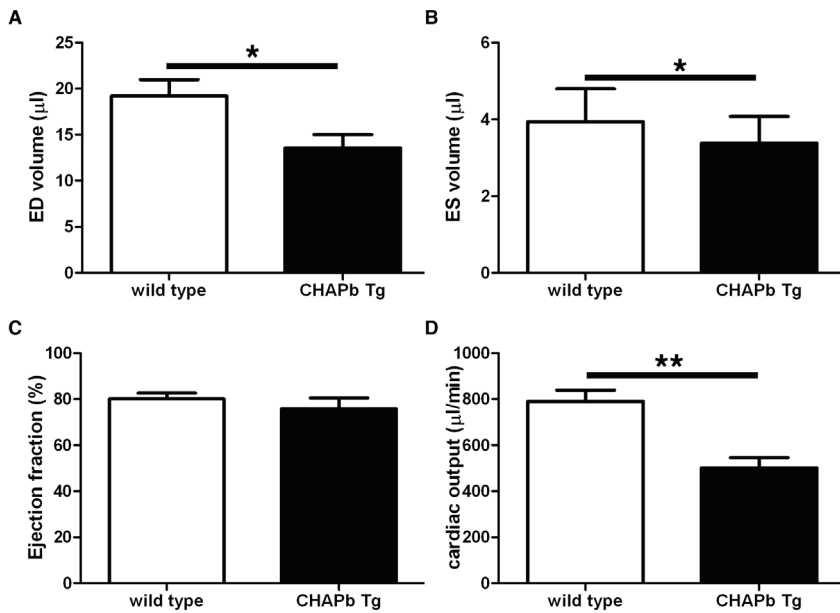
Supplemental figure 1: Hearts of CHAPb Tg founders that died spontaneously. A) Southern blot analysis of genomic wild type and CHAPb Tg DNA showing intermediate copy number in line 14 and high copy number in line 29, compared to wild type copy numbers. Hearts of CHAPb founder line 29 (left panels) and line 14 (right panels). B) Hearts showing enlarged atria and malformed ventricles. C) HE stained overview section showing enlarged atria and thickened ventricles. D). Higher magnification of the left ventricle. Scale bars in B 1 mm, in C 50  $\mu$ m.



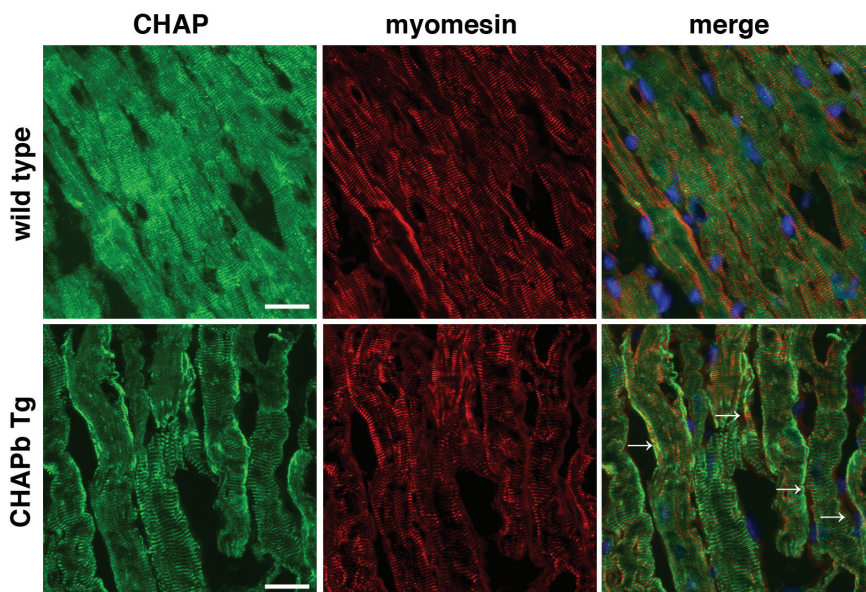
Supplemental figure 2: HE and Sirius red staining of CHAPb Tg hearts at one month of age. Wt (left panels) and CHAPb Tg (right panels) at 1 month of age (A-C). A) HE stained overview section. B) Higher magnification of left ventricle. C) Sirius red staining of the left ventricle. D and E) Volume of the left atrium (D) and right atrium (E) in wt (white bars) and CHAPb Tg (black bars) hearts. Scale bars 1 mm in A, 50  $\mu$ m in B, C.



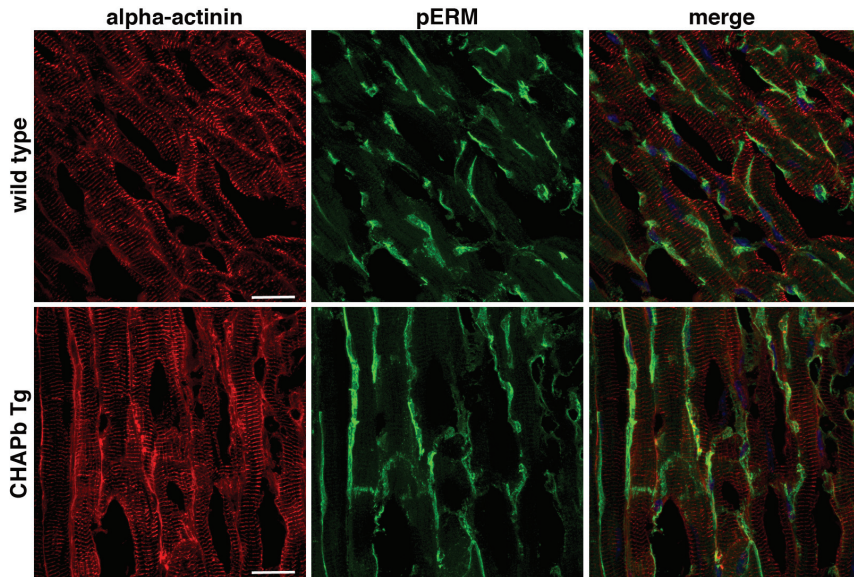
Supplemental figure 3: Expression of Connexin 40 and 43 at 1, 3 and 6 months. Immunohistochemical staining showing Connexin 40 (A and C) and 43 (B and D) expression in wt (left panels) and CHAPb Tg (right panels) left atria (A, B and upper panels of C and D) and right atria (lower panels of C and D) at one month (A and B) and 3 months of age (C and D) of age. qPCR analysis of *Connexin 43* (E and F) expression in the left (E) and right (F) atrium at 6 months of age. Scale bars 50  $\mu$ m.



Supplemental figure 4: Functional analysis of CHAPb Tg hearts. MRI measurements of the right ventricle of wt (white bars) and CHAPb Tg (black bars) animals at 6 months of age (A-F). ED volume (A), ES volume (B), ejection fraction (C) and cardiac output (D). ED (end diastolic), ES (end systolic) and LV (left ventricular).



Supplemental Figure 5: Expression of m-band marker myomesin is not affected in CHAPb Tg hearts. Hearts stained for CHAP (green) / myomesin (red), merge images are shown. CHAP is localized in the z-disc of cardiomyocytes of wt (upper panels) hearts. In cardiomyocytes of CHAPb Tg (lower panels) CHAP also stained stress fibers (arrows), which did not stain for myomesin. Scale bars: 20 μm.



Supplemental figure 6: Ectopic pERM expression in CHAPb Tg hearts. Wt (upper panels) and CHAPb Tg (lower panels) hearts at 6 months of age stained for pERM (green) and alpha-actinin (red). Nuclei are stained blue, merge images are shown. Scale bars: 20  $\mu$ m.

